Magnetization dependence on dynamic strain in ferromagnetic shape memory Ni–Mn–Ga

N. N. Sarawate[a] and M. J. Dapino[b]
Smart Vehicle Concepts Center, Department of Mechanical Engineering, The Ohio State University, Columbus, Ohio 43210, USA

(Received 12 May 2008; accepted 23 July 2008; published online 11 August 2008)

The characterization of commercial Ni–Mn–Ga for use as a dynamic deformation sensor is addressed. The flux density is experimentally determined as a function of cyclic strain loading at frequencies from 0.2 to 160 Hz. With increasing frequency, the stress versus strain response remains almost unchanged whereas the flux density versus strain response shows increasing hysteresis. This behavior indicates that twin-variant reorientation occurs in concert with the mechanical loading, whereas the rotation of magnetization vectors occurs with a delay as the loading frequency increases. The increasing magnetization hysteresis must be considered when utilizing the material in dynamic sensing applications. © *2008 American Institute of Physics*. [DOI: 10.1063/1.2969799]

A major advantage of ferromagnetic shape memory alloys (FSMAs) in the Ni–Mn–Ga system over the thermally activated SMAs is their ability to produce large strains of around 6% at high bandwidth in the kilohertz range. Because of the large magnetic field induced strain, extensive work has been done on the quasistatic actuation behavior (see review papers[1,2]). However, the characterization and modeling of Ni–Mn–Ga under dynamic mechanical or magnetic excitation has received only a limited attention. Henry *et al.*[3] presented measurements of magnetic field induced strains of up to 3% for drive field frequencies of up to 250 Hz and a linear model to describe the phase lag between strain and field and system resonance frequencies. Peterson *et al.*[4] presented dynamic actuation measurements on piezoelectrically assisted twin boundary motion in Ni–Mn–Ga. The acoustic stress waves produced by a piezoelectric actuator complement the externally applied fields and allow for reduced field strengths. Marioni *et al.*[5] presented pulsed magnetic field actuation of Ni–Mn–Ga for field pulses lasting up to 620 μs. The complete field induced strain was observed to occur in 250 μs, indicating the possibility of obtaining cyclic 6% strain for frequencies of up to 2000 Hz. Magnetization measurements were not reported in these studies as they usually are not of great interest for actuation applications. Faidley *et al.*[6] and Sarawate and Dapino[7] presented frequency response measurements of acceleration transmissibility using mechanical base excitation to investigate the effect of bias fields on the stiffness of Ni–Mn–Ga. However, the magnitude of base acceleration was not sufficient to induce twin boundary motion and associated magnetization changes.

The sensing effect in Ni–Mn–Ga refers to the action of external mechanical stress on the magnetic properties of the material. Only a few studies exist on the sensing effect of Ni–Mn–Ga (Ref. 8–12) as opposed to the actuation effect. Mullner *et al.*[8] experimentally studied strain induced changes in the flux density under external quasistatic loading at a constant field of 558 kA/m. Straka and Heczko[9] reported superelastic response for fields higher than 239 kA/m and established the interconnection between magnetization and strain. Heczko[11] further investigated this interconnection and proposed a simple energy model. Suorsa *et al.*[10] reported magnetization measurements for various discrete strain and field intensities ranging between 0% and 6% and 5 and 120 kA/m, respectively. Sarawate and Dapino[12] reported flux density change due to 6% strain input at bias fields ranging from 0 to 445 kA/m, and presented a continuum thermodynamics model[13] for the sensing effect. However, all of these studies are concerned with quasistatic magnetization responses, and an investigation on the effect of dynamic mechanical input on the magnetization of Ni–Mn–Ga is still lacking. Recently, Karaman *et al.*[14] reported voltage measurements in a pickup coil due to flux density change under dynamic strain loading of 4.9% at frequencies from 0.5 to 10 Hz from the viewpoint of energy harvesting using Ni–Mn–Ga. A maximum voltage of 280 mV was recorded for strain loading of 10 Hz at a bias field of 1.6 T. Their study presents the highest frequency of mechanical loading to date which induces twin boundary motion in Ni–Mn–Ga (10 Hz). However, the dependence of flux density on strain was not reported.

We experimentally determine the dependence of flux density and stress on dynamic strain at a bias field of 368 kA/m for frequencies of up to 160 Hz, with a view to determining the feasibility of using Ni–Mn–Ga as a dynamic deformation sensor. This bias field was determined as optimum for obtaining maximum reversible flux density change.[12] The measurements illustrate the dynamic behavior of twin boundary motion and magnetization rotation in Ni–Mn–Ga. As shown in Fig. 1, the experimental setup consists of a custom designed electromagnet and a uniaxial MTS 831 test frame. This frame is designed for cyclic fatigue loading, with special servo valves which allow precise stroke control up to 200 Hz.

A $6\times6\times10$ mm^3 single crystal Ni–Mn–Ga sample (AdaptaMat Ltd.) is placed in the center gap of an electromagnet. In the low-temperature martensite phase, the sample exhibits a free magnetic field induced deformation of 5.8% under a transverse field of 700 kA/m. The material is first

[a]Electronic mail: sarawate.1@osu.edu.
[b]Author to whom correspondence should be addressed. Electronic mail: dapino.1@osu.edu.

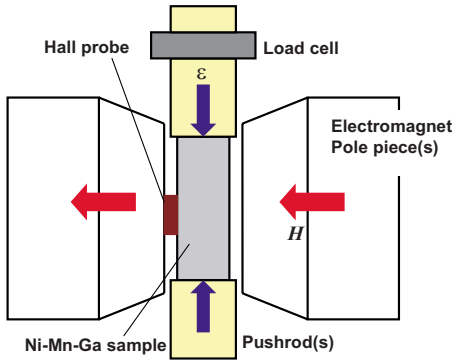

FIG. 1. (Color online) Experimental setup for dynamic magnetization measurements.

converted to a single field-preferred variant by applying a high field along the transverse (x) direction. The field is removed and the material is then slowly compressed 3.1% at a bias field of 368 kA/m applied in the x direction. While being exposed to the bias field, the sample is subjected to a cyclic uniaxial strain loading of 3% amplitude (peak to peak) along the longitudinal (y) direction at a desired frequency. This process is repeated for frequencies ranging between 0.2 and 160 Hz. The flux density inside the material is measured by a Hall probe placed in the gap between a magnet pole and a face of the sample. The Hall probe measures the net flux density along the x direction, from which the x-axis magnetization can be calculated. The compressive force is measured by a load cell, and the displacement is measured by a linear variable differential transducer. The data is collected using broadband instruments and recorded with a dynamic data acquisition software at a sampling frequency of 4096 Hz.

Figure 2 shows stress versus strain measurements for frequencies ranging from 4 to 160 Hz. The strain axis is biased around the initial strain of 3.1%. These plots show typical pseudoelastic minor loop behavior associated with single crystal Ni–Mn–Ga at a high bias field. With increasing compressive strain, the stress increases elastically, until a critical value is reached, after which twin boundary motion starts and the stress-preferred variants grow at the expense of the field-preferred variants. During unloading, the material exhibits pseudoelastic reversible behavior because the bias field of 368 kA/m causes the generation of field-preferred variants at the expense of stress-preferred variants.

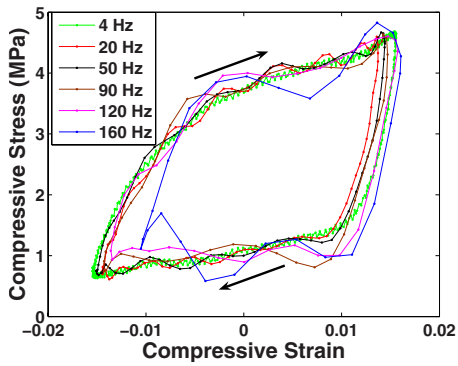

FIG. 2. (Color online) Stress vs strain for frequencies ranging from 4 to 160 Hz.

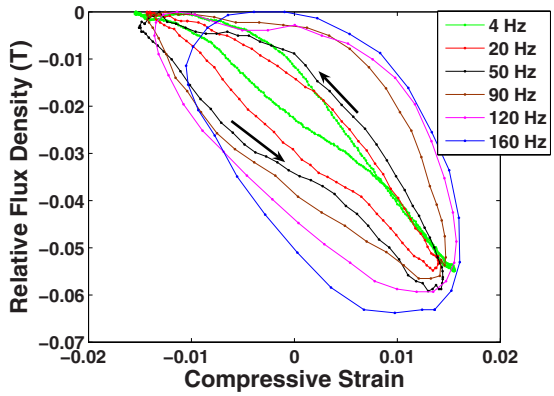

FIG. 3. (Color online) Relative change in flux density vs strain for frequencies ranging from 4 to 160 Hz.

The dependence of flux density on strain shown in Fig. 3 is of interest for sensing applications. The absolute value of flux density decreases with increasing compression. During compression, due to the high magnetocrystalline anisotropy of NiMnGa, the nucleation and growth of stress-preferred variants is associated with rotation of magnetization vectors into the longitudinal direction, which causes a reduction in the permeability and flux density in the transverse direction. At low frequencies of up to 4 Hz, the relationship between flux density and strain is almost linear with little hysteresis. This low-frequency behavior is consistent with some of the previous observations.[11,12,15] The net flux density change for a strain range of 3% is around 0.056 T (560 G) for almost all frequencies, which shows that the magnetization vectors rotate into the longitudinal direction by approximately the same amount for all the frequencies. The applied strain amplitude does not remain exactly at $\pm 1.5\%$ because the MTS controller is working at very low displacements ($\approx \pm 0.15$ mm) and high frequencies. Nevertheless, the strain amplitudes are maintained within a sufficiently narrow range ($\pm 8\%$) so that a consistent comparative study is possible for different frequencies.

With increasing frequency, the stress versus strain behavior remains relatively unchanged (Fig. 2). This indicates that twin-variant reorientation occurs in concert with the applied loading for the frequency range under consideration. This behavior is consistent with work by Marioni *et al.*[5] showing that twin boundary motion occurs in concert with the applied field for frequencies of up to 2000 Hz. On the other hand, the amount of hysteresis in the flux density versus strain curves shows a monotonic increase with increasing frequency (Fig. 3). The hysteresis loss in the stress versus strain plots is equal to the area enclosed by one cycle ($\oint \sigma d\varepsilon$); the loss in the flux density versus strain plots is obtained by multiplying the enclosed area ($\oint B d\varepsilon$) by a constant that has units of magnetic field.[16,17] Figure 4 shows the hysteresis loss for the stress versus strain and the flux density versus strain plots. The stress versus strain hysteresis is relatively flat over the frequency range considered. The flux density versus strain hysteresis is about ten times higher at 160 Hz than it is at 0.2 Hz. The energy loss, i.e., the area of the hysteresis loop is approximately linearly proportional to the frequency. The bias field of 368 kA/m is strong enough to ensure that the 180° domains disappear within each twin variant, hence each variant consists of a single magnetic domain throughout the cyclic loading process.[13] Therefore, the

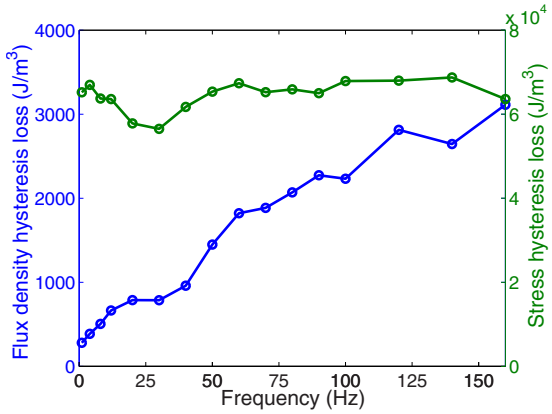

FIG. 4. (Color online) Hysteresis loss with frequency for stress vs strain and flux density vs strain plots.

only parameter affecting the magnetization hysteresis is the rotation angle of the magnetization vectors with respect to the easy c-axis. This angle is independent of the strain and variant volume fraction,[13] and is therefore a constant for the given bias field.

The process that leads to the observed magnetization dependence on strain is postulated to occur in three steps. (i) As the sample is compressed, twin-variant rearrangement occurs and the number of crystals with easy c-axis in the longitudinal (y) direction increases. The magnetization vectors remain attached to the c-axis, therefore the magnetization in these crystals is oriented along the y-direction. (ii) Subsequently, the magnetization vectors in these crystals rotate away from the c-axis to settle at a certain equilibrium angle defined by the competition between the Zeeman and magnetocrystalline anisotropy energies. This rotation process is proposed to occur according to the dynamics of a first order system. Time constants for first-order effects in Ni–Mn–Ga have been previously established for the time-dependent long-time strain response,[18,19] and strain response to pulsed field.[5] The time constant associated with pulse field response provides a measure of the dynamics of twin boundary motion, which is estimated to be around 157 μs.[5] In contrast, the time constant associated with magnetization rotation in our measurements is estimated to be around 1 ms. (iii) As the sample is unloaded, twin-variant rearrangement occurs due to the applied bias field. Crystals with the c-axis oriented along the y-direction rotate into the x-direction, and an increase in the flux density along the x-direction is observed. At low frequencies, magnetization rotation occurs in concert with twin-variant reorientation. As the frequency increases, the delay associated with the rotation of magnetization vectors into their equilibrium position increases, which leads to the increase in hysteresis seen in Fig. 3. The counterclockwise direction of the magnetization hysteresis loops implies that the dynamics of magnetization rotation occur as described in steps (i)–(iii). If the magnetization vectors had directly settled at the equilibrium angle without going through step (i), the direction of the hysteresis loops would have been clockwise.

We present the magnetization and stress response of single crystal Ni–Mn–Ga subjected to dynamic strain loading for frequencies from 0.2 to 160 Hz. This frequency range is significantly higher than the previous characterizations of Ni–Mn–Ga which presented frequencies from dc to 10 Hz. The rate of twin-variant reorientation remains unaffected by frequency, however the rate of rotation of magnetization vectors away from the easy c-axis is lower than the rate of loading and of twin-variant reorientation. This behavior can be qualitatively explained by the dynamics of a first order system associated with the rotation of magnetization vectors. The increasing flux density hysteresis with frequency could complicate the use of this material for dynamic sensing. However, the "sensitivity" of the material, i.e., net change in flux density per percentage strain input remains relatively unchanged ($\approx$190 G per % strain) with increasing frequencies. Thus the material retains the advantage of being a large-deformation, high-compliance sensor as compared to materials such as Terfenol-D (Ref. 12) at high frequencies. The significant magnetization change at high frequencies also illustrates the feasibility of using Ni–Mn–Ga for energy harvesting applications. To employ the material as a dynamic sensor or in energy harvesting applications, permanent magnets can be used instead of an electromagnet. The electromagnet provides the flexibility of turning the field on and off at a desired magnitude, but the permanent magnets provide an energy efficiency advantage. Further work is required to incorporate the rate dependencies in the existing analytical models[13] to understand the magnetization behavior at higher frequencies.

This research was supported by the National Science Foundation under grant CMS-0409512, Dr. Shih-Chi Liu program director, and a Smart Vehicle Concepts Center (www.SmartVehicleCenter.org) Graduate Fellowship.

[1] J. Kiang and L. Tong, J. Magn. Magn. Mater. **292**, 394 (2005).
[2] O. Soderberg, Y. Ge, A. Sozniov, S. Hannula, and V. K. Lindroos, Smart Mater. Struct. **14**, S223 (2005).
[3] C. Henry, P. Te11o, D. Bono, J. Hong, R. Wager, J. Dai, S. Allen, and R. O'Handley, Proc. SPIE **5053**, 207 (2003).
[4] B. Peterson, J. Feuchtwanger, J. Chambers, D. Bono, S. Hall, S. Allen, and R. O'Handley, J. Appl. Phys. **95**, 6963 (2004).
[5] M. A. Marioni, R. C. O'Handley, and S. M. Allen, Appl. Phys. Lett. **83**, 3966 (2003).
[6] L. Faidley, M. J. Dapino, G. Washington, and T. Lograsso, J. Intell. Mater. Syst. Struct. **17**, 123 (2006).
[7] N. Sarawate and M. Dapino, Proc. SPIE **6529**, 652916 (2007).
[8] P. Mullner, V. A. Chernenko, and G. Kostorz, Scr. Mater. **49**, 129 (2003).
[9] L. Straka and O. Heczko, IEEE Trans. Magn. **39**, 3402 (2003).
[10] I. Suorsa, E. Pagounis, and K. Ullakko, Appl. Phys. Lett. **84**, 4658 (2004).
[11] O. Heczko, J. Magn. Magn. Mater. **290**, 787 (2005).
[12] N. Sarawate and M. Dapino, Appl. Phys. Lett. **88**, 121923 (2006).
[13] N. Sarawate and M. Dapino, J. Appl. Phys. **101**, 123522 (2007).
[14] I. Karaman, B. Basaran, H. Karaca, A. Karsilayan, and Y. Chumlyakov, Appl. Phys. Lett. **90**, 172505 (2007).
[15] G. Li, Y. Liu, and B. Ngoi, Scr. Mater. **53**, 829 (2005).
[16] K. Uchino and S. Hirose, IEEE Trans. Magn. **48**, 307 (2001).
[17] A. Ercuta and I. Mihalca, J. Phys. D **35**, 2902 (2002).
[18] N. Glavatska and A. R. V. L'vov, J. Magn. Magn. Mater. **241**, 287 (2002).
[19] V. L'vov, O. Rudenko, and N. Glavatska, Phys. Rev. B **71**, 024421 (2005).